



Original Article

# Phase Transition in the Aligned Two-Higgs Doublet Model with the Goldstone Theorem Conserved

Dang Thi Minh Hue<sup>1,\*</sup>, Nguyen Tuan Anh<sup>2</sup>

<sup>1</sup>*Thuyloi University, 175 Tay Son, Kim Lien, Hanoi, Vietnam*

<sup>2</sup>*Electric Power University, 235 Hoang Quoc Viet, Hanoi, Vietnam*

Received 20<sup>th</sup> July 2025

Revised 4<sup>th</sup> September 2025; Accepted 2<sup>nd</sup> February 2026

**Abstract:** This paper studies the phase transition in the aligned two-Higgs doublet model by applying the Cornwall-Jackiw-Tomboulis effective potential in the double-bubble approximation. Its main feature is that the Goldstone theorem is restored in the model by adjusting the CJT effective potential, and the phase transition is of the second-order type, following the symmetry restoration scenario.

**Keywords:** Aligned two Higgs doublet model (A-THDM), Cornwall-Jackiw-Tomboulis (CJT), Standard Model (SM), Charge Conjugation Parity (CP), vacuum expectation values (VEV).

## 1. Introduction

In recent decades, the use of SM for research in particle physics has achieved numerous successes, including the successful explanation of the phenomena of particles in nature. Furthermore, the discovery of the Higgs boson by the Large Hadron Collider at the European Center for Nuclear Research (CERN) was an important milestone in particle physics in 2012 [1]. It has an extremely short lifetime and decays in many ways. It makes the Standard Model (SM) more perfect to describe the microscopic world as well as the existence of the universe. Its results show the existence of a new particle with a mass of approximately 125 GeV, which is compatible with the standard Higgs boson in the SM.

The Higgs boson is a new type of elementary particle with zero spin and has the smallest mass. It is not only an elementary particle that explains the spontaneous symmetry breaking, but also an important factor in ensuring the property of the unitary group of high-energy scattering between the boson W and the standard boson [1-7]. The Charge Conjugation Parity (CP) was investigated, in which the pure odd-

\* Corresponding author.

E-mail address: [dtmhue@tlu.edu.vn](mailto:dtmhue@tlu.edu.vn)

<https://doi.org/10.25073/2588-1124/vnumap.5047>

CP state cannot occur [8]. The Higgs boson's Yukawa binding was first observed by the work of ATLAS and CMS in 2018. Moreover, the data obtained by experiments in 2018 suggests that the second fermion is generated [9]. In general, results in the Lab related to the Higgs boson match the SM's predictions and expectations.

According to the SM, a particle's mass is created by its interaction with the Higgs field so that the vacuum expectation value (VEV) of this field is nonzero. This process depends on the type of Higgs potential. The particular configurations of the Higgs potential determine the types of phases that exist and the corresponding phase transitions of the matter. However, SM argues that neutrinos have no mass, while recent experimental studies have shown that they have mass [10]. In addition, a new measurement of the anomalous magnetic moment for Muon  $g-2$  shows that the scalar component of the Higgs field is not limited to a Higgs doublet, as the prediction of the SM that a doublet consists of only two particles at the same quantum state, but also has antiparallel spins [11]. So, the scalar neutral particle observed by LHC can only correspond to just one of many particles in the ensemble of scalar bosons. This Lab's results prove that the existence of a multi-Higgs model is suitable. Therefore, there are possibly many Higgs doublets, and each doublet can consist of some Higgs bosons [12]. Hence, the model describes Higgs bosons that must be consistent with the SM, and satisfy symmetries and invariant theorems for systems including many particles, including the Goldstone theorem.

Recently, there have been many papers dealing with the evidence of the existence of the Higgs boson and its properties following the multi-Higgs model in both experiment and theory, especially using the two-Higgs-doublet model (2HDM). It is one of the simplest multi-Higgs models, consisting of two doublets denoted by  $\Phi_1$  and  $\Phi_2$ , which have the same hypercharge  $Y$ , satisfying the  $SU(2)_L$  symmetry group. Using this model, many interesting phenomenological features are discovered, such as new sources of CP violation, dark matter candidates, axion phenomenology...[13]. It contains a second Higgs doublet with the same quantum numbers as the SM one. Specifically, the aligned two Higgs doublets model (A2HDM) is the 2HDM with the hypercharge  $Y$  equal to  $+1/2$ , in which each doublet consists of many Higgs bosons but produced by two types of Higgs particles, the standard Higgs ( $h$ ) having a mass approximately 125 GeV, and the other Higgs particle is heavier. In addition, the alignment limit of 2HDM can also be achieved without decoupling. However, for small  $\tan \beta$  values, it's usually attributed to accidental cancellations in the 2HDM potential. Note that  $\tan \beta = v_2/v_1$ , and the VEVs of the two scalar fields ( $\Phi_{1,2}$ ) of the two Higgs models. Furthermore, the research results about the alignment limit show that the SM alignment is often associated with the decoupling limit, in which all the non-standard Higgs bosons are assumed to be much heavier than the electroweak scale, so that the lightest CP-even scalar behaves just like the SM Higgs boson. Besides, it is found that there exist only three possible symmetry realizations of the scalar potential that predict natural alignment. Following this method, the heavy Higgs sector is quasi-degenerate as predicted. Gauge phobia is a generic feature in the alignment limit. Moreover, the current experimental constraints force the heavy Higgs sector to lie above the top-quark threshold. Thus, the dominant collider signal for this sector involves final states with third-generation quarks [14].

To study multi-Higgs models, an effective field theory formalism should be employed where the effects of the physics are written in terms of SM operators. One of the best candidates for studying loop expansions is the Cornwall–Jackiw–Tomboulis (CJT) formalism, a nonperturbative method for a multi-particle collective system, especially useful for phase transition studies [15]. Almost all physical theories are built on the symmetry principle. However, some symmetries are spontaneously broken when the Lagrangian is invariant under the transformation of symmetry groups, but the vacuum state is not invariant. This broken symmetry generates massless neutral scalar particles called Goldstone bosons, with the number obeying the Goldstone theorem [16].

In this paper, we use the CJT formalism to find the advanced CJT effective potential that preserves the Goldstone theorem and the order of phase transition for A2HDM.

This paper is organized as follows. In Sec.2, we present the research methods of the aligned two-Higgs doublet model. The results and discussions of this work are presented in Section 3. Section 4 is the conclusions.

## 2. Research Methods

In this work, we use the CJT formalism in the double-bubble approximation to preserve the Goldstone theorem for the aligned two-Higgs-doublet model (A2HDM) without the mixing of two Higgs bosons  $h$  and  $H_0$ . Then, the gap and Schwinger Dyson (SD) equations of state are used for numerical calculation self-consistently to find out the order of phase transition in this model. Its Lagrangian is given by:

$$L = (\partial^\mu \Phi_1)^\dagger (\partial_\mu \Phi_1) + (\partial^\mu \Phi_2)^\dagger (\partial_\mu \Phi_2) - V, \quad (1)$$

where  $V$  is the scalar potential of the model:

$$V = m_1^2 \Phi_1^\dagger \Phi_1 + m_2^2 \Phi_2^\dagger \Phi_2 - m_{12}^2 (\Phi_1^\dagger \Phi_2 + \Phi_2^\dagger \Phi_1) + \frac{\lambda_1}{2} (\Phi_1^\dagger \Phi_1)^2 + \frac{\lambda_2}{2} (\Phi_2^\dagger \Phi_2)^2 - \lambda_3 (\Phi_1^\dagger \Phi_1) (\Phi_2^\dagger \Phi_2) + \lambda_4 (\Phi_1^\dagger \Phi_2) (\Phi_2^\dagger \Phi_1) + \frac{\lambda_5}{2} [(\Phi_1^\dagger \Phi_2)^2 + (\Phi_2^\dagger \Phi_1)^2], \quad (2)$$

$m_1$  ( $m_2$ ) are the masses of Higgs doublets  $\Phi_1$  ( $\Phi_2$ ) including two types of Higgs boson;  $\lambda_i$  ( $i = 1; 2; 3; 4; 5$ ) are binding const between doublets in the model;  $m_{12}$  is specific to the combination of two doublets;  $u_1$  ( $u_2$ ) are the vacuum expectation values of  $\Phi_1$  ( $\Phi_2$ ).

In quantum field theory, the Goldstone theorem is preserved for all models describing the system. Therefore, it is necessary to have a formalism and method to approach the multi-Higgs model so that the Goldstone theorem is valid. Hence, it must have a suitable formalism and methodology to renormalize the theory.

In this research, we chose the physical unit system in which  $c = 1, \hbar = 1$  then  $1eV \simeq 11065K$ , and assume that not only is CP conserved for scalar components, leading to all coefficients being real, but also only one  $Z_2$  symmetry happens in the model:  $\Phi_1 \rightarrow -\Phi_1$  or  $\Phi_2 \rightarrow -\Phi_2$  is forbidden by quartic terms in odd numbers of  $\Phi_i$ .

Since the Eq (1) is invariant under the SU(2) group transformation, the  $Z_2$  symmetry is easily broken by quadratic terms  $m_{12}^2$ . To get only one scalar doublet that can couple to a given right-handed fermion, the model (1) obeys specific discrete  $Z_2$  symmetries. Thus, there must exist 3 Goldstone bosons in this model, according to the Goldstone theorem. Hence, we first build the CJT effective potential to preserve the Goldstone theorem for A2HDM by transforming all matrices of Higgs components to be diagonal. Then, we perform numerical research to consider its phase transition.

## 3. Results and Discussion

### 3.1. Results

Firstly, we use field transformation:

$$\Phi_1 \rightarrow \frac{1}{\sqrt{2}} \begin{pmatrix} \Phi_1^+ \\ \zeta_1 + u_1 + i\chi_1 \end{pmatrix}, \Phi_2 \rightarrow \frac{1}{\sqrt{2}} \begin{pmatrix} \Phi_2^+ \\ \zeta_2 + u_2 + i\chi_2 \end{pmatrix}, \quad (3)$$

where  $\rho(\zeta)$  are the real scalar components;  $\eta(\chi)$  are the virtual components of the Higgs field, and

$$\langle \Phi_1 \rangle \rightarrow \frac{1}{\sqrt{2}} \begin{pmatrix} 0 \\ u_1 \end{pmatrix}, \langle \Phi_2 \rangle \rightarrow \frac{1}{\sqrt{2}} \begin{pmatrix} 0 \\ u_2 \end{pmatrix}, \quad (4)$$

are VEVs of two Higgs doublets. The VEVs at  $T = 0$  are defined by  $v_i = u_i|_{T=0}$  (5)

relating to the VEV in the SM,  $v \simeq 246$  GeV as a relationship below

$$u^2 = u_1^2 + u_2^2, v = u|_{T=0} \quad (6)$$

and the angle  $\beta$  is the ratio of  $u_1$  and  $u_2$ :  $t_\beta = \tan \beta = \frac{u_2}{u_1}$ . (7)

Inputting in terms of (1) and (2) leads to obtaining the Lagrangian specific to the interaction creating mass for the Higgs boson in the model:

$$L_{\text{mass}} = - \left[ \frac{m_{12}^2}{c_\beta s_\beta} \left( -\frac{(\lambda_4 + \lambda_5)u^2}{2} \right) \right] (G^{-1} H^{-1}) \begin{pmatrix} 0 & 0 \\ 0 & 1 \end{pmatrix} \begin{pmatrix} G^+ \\ H^+ \end{pmatrix}, \quad (8)$$

$$- \frac{1}{2} (h H_0) \begin{pmatrix} M_{11} & M_{12} \\ M_{21} & M_{22} \end{pmatrix} \begin{pmatrix} h \\ H_0 \end{pmatrix} - \frac{1}{2} \left( \frac{m_{12}^2}{c_\beta s_\beta} - \lambda_5 u^2 \right) (G_0 A) \begin{pmatrix} 0 & 0 \\ 0 & 1 \end{pmatrix} \begin{pmatrix} G_0 \\ A \end{pmatrix}$$

, in which  $G_0, G^\pm$  are Goldstone bosons, and the boson  $A$  is the Higgs boson, which does not obey the odd component of CP:

$$G^\pm = (G_1 \pm iG_2) / \sqrt{2}; H^\pm = (H_1 \pm iH_2) / \sqrt{2}, \quad (9)$$

$$M_{11} = \lambda_1 c_\beta^4 + \lambda_2 s_\beta^4 + 2(\lambda_3 + \lambda_4 + \lambda_5) c_\beta^2 s_\beta^2, M_{12} = -c_\beta s_\beta \left[ \lambda_1 c_\beta^2 - \lambda_2 s_\beta^2 - (\lambda_3 + \lambda_4 + \lambda_5)(c_\beta^2 - s_\beta^2) \right], \quad (10)$$

$$M_{21} = -c_\beta s_\beta \left[ \lambda_2 c_\beta^2 - \lambda_1 s_\beta^2 - (\lambda_3 + \lambda_4 + \lambda_5)(s_\beta^2 - c_\beta^2) \right], M_{22} = \frac{m_{12}^2}{c_\beta s_\beta} + \left[ \lambda_1 + \lambda_2 - 2(\lambda_3 + \lambda_4 + \lambda_5) \right] u^2 c_\beta^2 s_\beta^2.$$

$$c_\beta = \cos \beta, s_\beta = \sin \beta.$$

The condition below must be valid to prevent the mixing of  $h$  and  $H_0$  [15].

$$\lambda_1 c_\beta^2 - \lambda_2 s_\beta^2 = (\lambda_3 + \lambda_4 + \lambda_5)(c_\beta^2 - s_\beta^2). \quad (11)$$

Eq.(10) is a non-separable condition for 2HDM at the tree level.

In the Higgs basis,

$$\Phi_h = \begin{pmatrix} G^+ \\ (h + u + iG_0) / \sqrt{2} \end{pmatrix}, \Phi_H = \begin{pmatrix} H^+ \\ (H_0 + iA) / \sqrt{2} \end{pmatrix}, \quad (12)$$

$$\begin{pmatrix} \Phi_1 \\ \Phi_2 \end{pmatrix} = R_\beta \begin{pmatrix} \Phi_h \\ \Phi_H \end{pmatrix}, R_\beta = \begin{pmatrix} c_\beta & -s_\beta \\ s_\beta & c_\beta \end{pmatrix}, \begin{pmatrix} \rho_1 \\ \rho_2 \end{pmatrix} = R_\beta \begin{pmatrix} G_1 \\ H_1 \end{pmatrix}, \begin{pmatrix} \eta_1 \\ \mu_2 \end{pmatrix} = R_\beta \begin{pmatrix} G_2 \\ H_2 \end{pmatrix}, \begin{pmatrix} \chi_1 \\ \chi_2 \end{pmatrix} = R_\beta \begin{pmatrix} G_0 \\ A \end{pmatrix}, \begin{pmatrix} \zeta_1 \\ \zeta_2 \end{pmatrix} = R_\beta \begin{pmatrix} h \\ H_0 \end{pmatrix}, \quad (13)$$

$$u^2 = u_1^2 + u_2^2, u_1 = u \cos \beta; u_2 = u \sin \beta, \quad (14)$$

yielding

$$\begin{aligned}
 L_{\text{mass}} = & -\frac{1}{2} \left[ \tilde{m}_1^2 + \frac{\tilde{\lambda}_1 u^2}{2} \right] (2G^+ G^- + G_0^2) - \frac{1}{2} \left[ \tilde{m}_2^2 + \frac{\tilde{\lambda}_3 u^2}{2} + \frac{\tilde{\lambda}_4 u^2}{2} - \frac{\tilde{\lambda}_5 u^2}{2} \right] A^2 \\
 & - \frac{1}{2} \left[ \tilde{m}_2^2 + \frac{\tilde{\lambda}_3 u^2}{2} \right] (H^+ H^-) - \frac{1}{2} \left[ \tilde{m}_1^2 + \frac{3\tilde{\lambda}_1 u^2}{2} \right] h^2 - \frac{1}{2} \left[ \tilde{m}_2^2 + \frac{\tilde{\lambda}_3 u^2}{2} + \frac{\tilde{\lambda}_4 u^2}{2} + \frac{\tilde{\lambda}_5 u^2}{2} \right] H_0^2 \\
 & - \left[ -\tilde{m}_{12}^2 + \frac{\tilde{\lambda}_6 u^2}{2} \right] (G_1 H_1 + G_2 H_2 + G_0 A) - \left[ -\tilde{m}_{12}^2 + \frac{3\tilde{\lambda}_6 u^2}{2} \right] h H_0,
 \end{aligned} \tag{15}$$

where

$$\begin{aligned}
 \tilde{m}_1^2 &= m_1^2 c_\beta^2 + m_2^2 s_\beta^2 - 2m_{12}^2 s_\beta c_\beta, \tilde{m}_2^2 = m_1^2 s_\beta^2 + m_2^2 c_\beta^2 + 2m_{12}^2 s_\beta c_\beta, \\
 \tilde{m}_{12}^2 &= (m_1^2 - m_2^2) s_\beta c_\beta + 2m_{12}^2 (c_\beta^2 - s_\beta^2), \tilde{\lambda}_1 = \lambda_1 c_\beta^4 + \lambda_2 s_\beta^4 + 2(\lambda_3 + \lambda_4 + \lambda_5) s_\beta^2 c_\beta^2, \\
 \tilde{\lambda}_2 &= \lambda_1 s_\beta^4 + \lambda_2 c_\beta^4 + 2(\lambda_3 + \lambda_4 + \lambda_5) s_\beta^2 c_\beta^2, \tilde{\lambda}_3 = (\lambda_1 + \lambda_2 - 2\lambda_4 - 2\lambda_5) s_\beta^2 c_\beta^2 + \lambda_3 (c_\beta^4 + s_\beta^4), \\
 \tilde{\lambda}_4 &= (\lambda_1 + \lambda_2 - 2\lambda_3 - 2\lambda_5) s_\beta^2 c_\beta^2 + \lambda_4 (c_\beta^4 + s_\beta^4), \tilde{\lambda}_5 = (\lambda_1 + \lambda_2 - 2\lambda_3 - 2\lambda_4) s_\beta^2 c_\beta^2 + \lambda_5 (c_\beta^4 + s_\beta^4), \\
 \tilde{\lambda}_6 &= -(\lambda_1 c_\beta^2 - \lambda_2 s_\beta^2) s_\beta c_\beta + (\lambda_3 + \lambda_4 + \lambda_5) s_\beta c_\beta (c_\beta^4 - s_\beta^4), \\
 \tilde{\lambda}_7 &= -(\lambda_1 s_\beta^2 - \lambda_2 c_\beta^2) s_\beta c_\beta + (\lambda_3 + \lambda_4 + \lambda_5) s_\beta c_\beta (s_\beta^4 - c_\beta^4).
 \end{aligned} \tag{16}$$

The alignment condition to prevent the mixing of  $h$  and  $H_0$  is

$$\tilde{m}_{12} = 0 \rightarrow \lambda_6 = 0. \tag{17}$$

Based on the CJT formalism and performing similar steps as the work of [15], obtained the CJT effective potential at finite temperature for A2HDM in the improved double-bubble approximation as follows:

$$\begin{aligned}
 V^{CJT} = & \frac{\tilde{m}_1^2}{2} u^2 + \frac{\tilde{\lambda}_1}{8} u^4 + \int_T \text{tr} \left\{ \ln D_c^{-1}(k) + \frac{1}{2} \ln D_a^{-1}(k) \right\} + \int_T \text{tr} \left\{ \frac{1}{2} \ln D_h^{-1}(k) \right\} + \int_T \text{tr} \left\{ \frac{1}{2} D_{0h}^{-1}(k; u) D_h(k) - 211 \right\} \\
 & + \int_T \text{tr} \left\{ D_{0c}^{-1}(k; u) D_c(k) + \frac{1}{2} D_{0a}^{-1}(k; u) D_a(k) \right\} + \frac{\tilde{\lambda}_1}{8} (2P_{c11} + P_{a11} + P_{h11})^2 + \frac{\tilde{\lambda}_2}{8} (2P_{c22} + P_{a22} + P_{h22})^2 + \\
 & \frac{\tilde{\lambda}_3}{4} (2P_{c11} + P_{a11} + P_{h11})(2P_{c22} + P_{a22} + P_{h22}) + \frac{\tilde{\lambda}_4}{4} [(P_{a11} + P_{h11})(P_{a22} + P_{h22}) + 2P_{c11} P_{c22}] + \frac{\tilde{\lambda}_5}{4} (P_{a11} - P_{h11})(P_{a22} - P_{h22}),
 \end{aligned} \tag{18}$$

where

$$P_{\alpha ij} = \int_T iD_{\alpha ij}(k), \alpha = c, a, h; i, j = 1, 2, \int_\beta f(k) = T \sum_{n=-\infty}^{+\infty} \int \frac{d^3 k}{(2\pi)^3} f(\omega_n, \vec{k}), \omega_n = 2\pi nT. \tag{19}$$

, and the inverse of tree-level propagators read

$$iD_{0c}^{-1}(k, u_i) = \begin{pmatrix} \omega^2 - \vec{k}^2 - \tilde{m}_1^2 - \frac{\tilde{\lambda}_1 u^2}{2} & 0 \\ 0 & \omega^2 - \vec{k}^2 - \tilde{m}_2^2 - \frac{\tilde{\lambda}_3 u^2}{2} \end{pmatrix}, \tag{20}$$

$$iD_{0a}^{-1}(k, u_i) = \begin{pmatrix} \omega^2 - \vec{k}^2 - \tilde{m}_1^2 - \frac{\tilde{\lambda}_4 u^2}{2} & 0 \\ 0 & \omega^2 - \vec{k}^2 - \tilde{m}_2^2 - \frac{\tilde{\lambda}_3 + \tilde{\lambda}_4 - \tilde{\lambda}_5}{2} u^2 \end{pmatrix}, \tag{21}$$

$$iD_{0h}^{-1}(k, u_i) = \begin{pmatrix} \omega^2 - \vec{k}^2 - \tilde{m}_1^2 - \frac{3\tilde{\lambda}_4 u^2}{2} & 0 \\ 0 & \omega^2 - \vec{k}^2 - \tilde{m}_2^2 - \frac{\tilde{\lambda}_3 + \tilde{\lambda}_4 + \tilde{\lambda}_5}{2} u^2 \end{pmatrix} \tag{22}$$

By taking traces of the matrices (20)-(22) in the momentum space, we get the expressions of the Nambu-Goldstone energy modes existing in the model:

$$\begin{aligned} E_1 &= \pm \sqrt{\left(\omega^2 - \vec{k}^2 - \tilde{m}_1^2 - \frac{\tilde{\lambda}_4 u^2}{2}\right)\left(\omega^2 - \vec{k}^2 - \tilde{m}_2^2 - \frac{\tilde{\lambda}_3 u^2}{2}\right)}, \\ E_2 &= \pm \sqrt{\left(\omega^2 - \vec{k}^2 - \tilde{m}_1^2 - \frac{\tilde{\lambda}_4 u^2}{2}\right)\left(\omega^2 - \vec{k}^2 - \tilde{m}_2^2 - \frac{\tilde{\lambda}_3 + \tilde{\lambda}_4 - \tilde{\lambda}_5}{2} u^2\right)}, \\ E_3 &= \pm \sqrt{\left(\omega^2 - \vec{k}^2 - \tilde{m}_1^2 - \frac{3\tilde{\lambda}_4 u^2}{2}\right)\left(\omega^2 - \vec{k}^2 - \tilde{m}_2^2 - \frac{\tilde{\lambda}_3 + \tilde{\lambda}_4 + \tilde{\lambda}_5}{2} u^2\right)}. \end{aligned} \tag{23}$$

The expression (23) shows that 6 Goldstone bosons are produced, or the Goldstone theorem is violated. Hence, to preserve it, we adjust the CJT potential (18) by adding  $\Delta V^{CJT}$  :

$$\begin{aligned} \tilde{V}^{CJT} &= V^{CJT} + \Delta V^{CJT}, \Delta V^{CJT} = x\tilde{\lambda}_1(2P_{c11} + P_{a11})P_{h11} + y_1\tilde{\lambda}_4P_{c11}(P_{a22} + P_{h22}) \\ &+ 2y_2\tilde{\lambda}_4P_{c11}P_{c22} + z_1\tilde{\lambda}_5(P_{a11} - P_{h11})(P_{a22} - P_{h22}) + z_2\tilde{\lambda}_5P_{c11}(P_{a22} - P_{h22}) \end{aligned} \tag{24}$$

, and  $x, y, z$  in (24) must be:

$$x = y_1 = 1/2, y_2 = z_1 = z_2 = -1/2. \tag{25}$$

It leads to

$$\begin{aligned} \tilde{V}^{CJT} &= \frac{\tilde{m}_1^2}{2}u^2 + \frac{\tilde{\lambda}_1}{8}u^4 + \int_T tr \left\{ \ln D_c^{-1} + \frac{1}{2} \ln D_a^{-1} + \frac{1}{2} \ln D_h^{-1} \right\} + \int_T tr \left\{ D_{0c}^{-1}D_c + \frac{1}{2}D_{0a}^{-1}D_a + \frac{1}{2}D_{0h}^{-1}D_h(k) - 211 \right\} + \\ &\frac{\tilde{\lambda}_1}{8} \left[ (2P_{c11} + P_{a11} + P_{h11})^2 + 4(2P_{c11} + P_{a11})P_{h11} \right] + \frac{\tilde{\lambda}_3}{4}(2P_{c11} + P_{a11} + P_{h11})(2P_{c22} + P_{a22} + P_{h22}) + \\ &\frac{\tilde{\lambda}_2}{8}(2P_{c22} + P_{a22} + P_{h22})^2 + \frac{\tilde{\lambda}_4}{4}(2P_{c11} + P_{a11} + P_{h11})(P_{a22} + P_{h22}) - \frac{\tilde{\lambda}_5}{4}(2P_{c11} + P_{a11} - P_{h11})(P_{a22} - P_{h22}), \end{aligned} \tag{26}$$

where the inverse propagators at the tree-level approximation become

$$\begin{aligned} iD_c^{-1}(k, u_i) &= & iD_a^{-1}(k, u_i) &= & iD_h^{-1}(k, u_i) &= \\ \begin{pmatrix} \omega^2 - \vec{k}^2 - \tilde{M}_{c1}^2 & 0 \\ 0 & \omega^2 - \vec{k}^2 - \tilde{M}_{c2}^2 \end{pmatrix}, & \begin{pmatrix} \omega^2 - \vec{k}^2 - \tilde{M}_{a1}^2 & 0 \\ 0 & \omega^2 - \vec{k}^2 - \tilde{M}_{a2}^2 \end{pmatrix}, & \begin{pmatrix} \omega^2 - \vec{k}^2 - \tilde{M}_{h1}^2 & 0 \\ 0 & \omega^2 - \vec{k}^2 - \tilde{M}_{h2}^2 \end{pmatrix}, \end{aligned} \tag{27}$$

in which

$$\begin{aligned} \tilde{M}_{c1}^2 = 0, \tilde{M}_{c2}^2 = \tilde{m}_2^2 + \frac{\tilde{\lambda}_3 u^2}{2} + \sum_{c2}^{\sim}, \tilde{M}_{a1}^2 = 0, \tilde{M}_{a2}^2 = \tilde{m}_2^2 + \frac{(\tilde{\lambda}_3 + \tilde{\lambda}_4 - \tilde{\lambda}_5)u^2}{2} + \sum_{a2}^{\sim}, \\ \tilde{M}_{h1}^2 = \tilde{m}_1^2 + \frac{3\tilde{\lambda}_3 u^2}{2} + \sum_{h1}^{\sim}, \tilde{M}_{h2}^2 = \tilde{m}_2^2 + \frac{(\tilde{\lambda}_3 + \tilde{\lambda}_4 + \tilde{\lambda}_5)u^2}{2} + \sum_{h2}^{\sim}. \end{aligned} \quad (28)$$

$$\begin{aligned} \sum_{c2}^{\sim} &= \frac{\tilde{\lambda}_2}{2}(2P_{c22} + P_{a22} + P_{h22}) + \frac{\tilde{\lambda}_3}{2}(2P_{c11} + P_{a11} + P_{h11}), \\ \sum_{a2}^{\sim} &= \frac{\tilde{\lambda}_2}{2}(2P_{c22} + P_{a22} + P_{h22}) + \frac{\tilde{\lambda}_3 + \tilde{\lambda}_4}{2}(2P_{c11} + P_{a11} + P_{h11}) - \frac{\tilde{\lambda}_5}{2}(2P_{c11} + P_{a11} - P_{h11}), \\ \sum_{h1}^{\sim} &= \frac{\tilde{\lambda}_1}{2}(6P_{c11} + 3P_{a11} + P_{h11}) + \frac{\tilde{\lambda}_3}{2}(2P_{c22} + P_{a22} + P_{h22}) + \frac{\tilde{\lambda}_4}{2}(P_{a22} + P_{h22}), \\ \sum_{h2}^{\sim} &= \frac{\tilde{\lambda}_2}{2}(2P_{c22} + P_{a22} + P_{h22}) + \frac{\tilde{\lambda}_3 + \tilde{\lambda}_4}{2}(2P_{c11} + P_{a11} + P_{h11}) + \frac{\tilde{\lambda}_5}{2}(2P_{c11} + P_{a11} - P_{h11}). \end{aligned} \quad (29)$$

We obtain the expressions of the Nambu Goldstone energy mode in the momentum space by taking traces of the matrices (27):

$$\begin{aligned} E_1 &= \sqrt{(\omega^2 - \vec{k}^2)(\omega^2 - \vec{k}^2 - \tilde{M}_{c2}^2)}, \\ E_2 &= \sqrt{(\omega^2 - \vec{k}^2)(\omega^2 - \vec{k}^2 - \tilde{M}_{a2}^2)}, \\ E_3 &= \sqrt{(\omega^2 - \vec{k}^2 - \tilde{M}_{h1}^2)(\omega^2 - \vec{k}^2 - \tilde{M}_{h2}^2)}. \end{aligned} \quad (30)$$

Thus, Eq. (30) shows that 3 Goldstone bosons exist in the model after the CJT potential is Goldstoned. That means the Goldstone theorem is preserved for A2HDM.

Next, we investigate the order of phase transition in the A2HDM by considering the dependence of its VEVs on the temperature. To achieve this aim, must find the expressions describing the VEVs versus temperature. Hence, we use the physical requirements for the basic state of the model. That means the physical conditions have to satisfy:

$$\frac{\delta \tilde{V}^{CJT}}{\delta u} = 0; \frac{\delta \tilde{V}^{CJT}}{\delta D_\alpha} = 0 \quad (31)$$

, so it leads to the GAP equation and Schrödinger-Dyson (SD) equation:

$$\tilde{m}_1^2 + \frac{\tilde{\lambda}_1}{2}u^2 + \sum_u = 0, \quad (32)$$

$$iD_\alpha^{-1}(k) = iD_{0\alpha}^{-1}(k; u) - \sum_\alpha, \alpha = c, a, h, \quad (33)$$

where

$$\sum_u = \frac{\tilde{\lambda}_1}{2}(2P_{c11} + P_{a11} + 3P_{h11}) + \frac{\tilde{\lambda}_3}{2}(2P_{c22} + P_{a22} + 3P_{h22}) + \frac{\tilde{\lambda}_4}{2}(P_{a22} + P_{h22}) - \frac{\tilde{\lambda}_5}{2}(P_{a22} - P_{h22}) \quad (34)$$

$$iD_\alpha^{-1}(k) = \begin{pmatrix} \omega^2 - \vec{k}^2 - M_{1\alpha}^2 & 0 \\ 0 & \omega^2 - \vec{k}^2 - M_{2\alpha}^2 \end{pmatrix}, \begin{pmatrix} \sum_{1\alpha} & 0 \\ 0 & \sum_{2\alpha} \end{pmatrix}, \quad (35)$$

and

$$\begin{aligned}
 \sum_{1c} &= \frac{\tilde{\lambda}_1}{2}(2P_{c11} + P_{a11} + P_{h11}) + \frac{\tilde{\lambda}_3}{2}(2P_{c22} + P_{a22} + P_{h22}) + \tilde{\lambda}_4 P_{c22}, \\
 \sum_{2c} &= \frac{\tilde{\lambda}_2}{2}(2P_{c22} + P_{a22} + P_{h22}) + \frac{\tilde{\lambda}_3}{2}(2P_{c11} + P_{a11} + P_{h11}) + \tilde{\lambda}_4 P_{c11}, \\
 \sum_{1a} &= \frac{\tilde{\lambda}_1}{2}(2P_{c11} + P_{a11} + P_{h11}) + \frac{\tilde{\lambda}_3}{2}(2P_{c22} + P_{a22} + P_{h22}) + \frac{\tilde{\lambda}_4}{2}(P_{a22} + P_{h22}) + \frac{\tilde{\lambda}_5}{2}(P_{a22} - P_{h22}), \\
 \sum_{2a} &= \frac{\tilde{\lambda}_2}{2}(2P_{c22} + P_{a22} + P_{h22}) + \frac{\tilde{\lambda}_3}{2}(2P_{c11} + P_{a11} + P_{h11}) + \frac{\tilde{\lambda}_4}{2}(P_{a11} + P_{h11}) + \frac{\tilde{\lambda}_5}{2}(P_{a11} - P_{h11}), \\
 \sum_{1h} &= \frac{\tilde{\lambda}_1}{2}(2P_{c11} + P_{a11} + P_{h11}) + \frac{\tilde{\lambda}_3}{2}(2P_{c22} + P_{a22} + P_{h22}) + \frac{\tilde{\lambda}_4}{2}(P_{a22} + P_{h22}) - \frac{\tilde{\lambda}_5}{2}(P_{a22} - P_{h22}), \\
 \sum_{2h} &= \frac{\tilde{\lambda}_2}{2}(2P_{c22} + P_{a22} + P_{h22}) + \frac{\tilde{\lambda}_3}{2}(2P_{c11} + P_{a11} + P_{h11}) + \frac{\tilde{\lambda}_4}{2}(P_{a11} + P_{h11}) - \frac{\tilde{\lambda}_5}{2}(P_{a11} - P_{h11}).
 \end{aligned} \tag{36}$$

The SD equations (33) can be reduced to the following system of equations that describe the effective masses of the Higgs boson in the model.

$$\begin{aligned}
 M_{1c}^2 &= \tilde{m}_1^2 + \frac{\tilde{\lambda}_1 u^2}{2} + \sum_{1c}, M_{2c}^2 = \tilde{m}_2^2 + \frac{\tilde{\lambda}_3 u^2}{2} + \sum_{2c} \\
 M_{1a}^2 &= \tilde{m}_1^2 + \frac{\tilde{\lambda}_1 u^2}{2} + \sum_{1a}, M_{2a}^2 = \tilde{m}_2^2 + \frac{\tilde{\lambda}_3 u^2}{2} + \frac{\tilde{\lambda}_4 u^2}{2} - \frac{\tilde{\lambda}_5 u^2}{2} + \sum_{2a} \\
 M_{1h}^2 &= \tilde{m}_1^2 + \frac{3\tilde{\lambda}_1 u^2}{2} + \sum_{1h}, M_{2h}^2 = \tilde{m}_2^2 + \frac{\tilde{\lambda}_3 u^2}{2} + \frac{\tilde{\lambda}_4 u^2}{2} + \frac{\tilde{\lambda}_5 u^2}{2} + \sum_{2h}
 \end{aligned} \tag{37}$$

To perform a numerical study of phase transition in the A2HDM, we must choose a small value of  $\tan\beta$  in the region from 1 to 20 to avoid accidental cancellations in the 2HDM potential and get above the top-quark threshold:  $\lambda_4 = \lambda_5 = 0, \tilde{m}_{12} = 0$  [15]. The mass difference between the heavy Higgs states should be small, and their scan intervals are therefore chosen to be identical in the range of experiments as follows [18]:

$$m_h = 125.09 GeV, m_A \approx m_{H^0} \approx m_{H^\pm} = 200 GeV, \tilde{m}_2 = 100 GeV; \tan\beta = 2; v = 246 GeV. \tag{38}$$

Hence,

$$\tilde{\lambda}_1 v^2 = m_h^2, \tilde{\lambda}_2 = \frac{-\tilde{\lambda}_1 (c_\beta^8 + c_\beta^6 s_\beta^2 - 12c_\beta^4 s_\beta^4 + c_\beta^2 s_\beta^6 + s_\beta^8)}{c_\beta^2 s_\beta^2 (5c_\beta^4 - 2c_\beta^2 s_\beta^2 + 5s_\beta^4)} + \frac{2(\tilde{\lambda}_3 + \tilde{\lambda}_4 + \tilde{\lambda}_5)(c_\beta^8 - c_\beta^6 s_\beta^2 - c_\beta^2 s_\beta^6 + s_\beta^8)}{c_\beta^2 s_\beta^2 (5c_\beta^4 - 2c_\beta^2 s_\beta^2 + 5s_\beta^4)} \tag{39}$$

$$\tilde{\lambda}_3 v^2 = 2m_{H^\pm}^2 - 2\tilde{m}_2^2, \tilde{m}_{12}^2 = 0, \tilde{\lambda}_4 v^2 = 2m_{H^0}^2 + m_A^2 - 2m_{H^\pm}^2 = 0, \tilde{\lambda}_5 v^2 = m_{H^0}^2 - m_A^2, \lambda_6 = 0, \tilde{m}_1^2 = -\frac{m_h^2}{2}.$$

Thus, the model with the chosen parameters as Eq. (38) satisfies the alignment condition (17). By solving the GAP equations (31), Eq. (37), and combined with Eq. (38,39), we obtain the evolution of VEV for Higgs bosons versus temperature plotted in Figure 1. The results in Fig.1 indicate that a phase transition happens in A2HDM at  $T = T_c \approx 237 GeV$ . It is the second-order phase transition for both doublets and follows the symmetry restoration scenario [17]. Because all VEVs are non-zero at  $T = 0$ , they lightly decrease to zero as the temperature increases, and they all get zero value at  $T = T_c$ . That means the model changes from the broken symmetry phase to the symmetry restoration phase when  $T = T_c$ . This feature agrees with the data of the LHC obtained in 2012 and 2024 [3, 5].

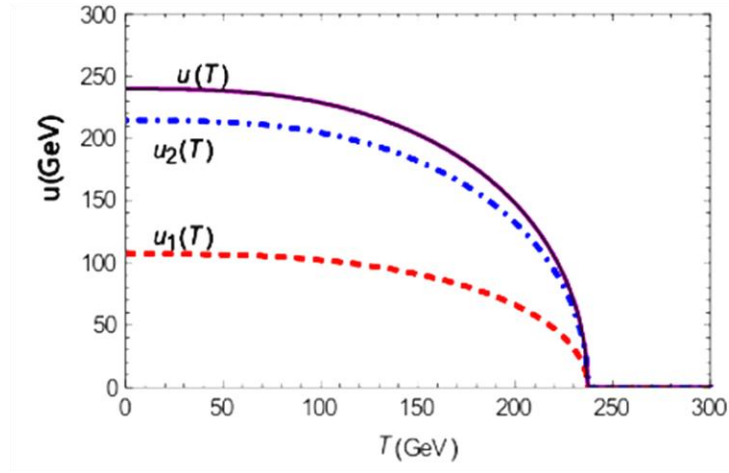


Figure 1. The dependence of VEVs on temperature  $T$  with the chosen parameters as Eq. (38).

Lastly, to confirm the second-order phase transition in the model, we use the imaginary time formalism to calculate the integral terms in the CJT effective potential at finite temperatures.

$$t \rightarrow i\tau, \text{ with } 0 \leq \tau \leq 1/T \text{ and } \int \frac{d^4 k}{(2\pi)^3} f(k) = iT \sum_{n=-\infty}^{+\infty} \int \frac{d^3 k}{(2\pi)^3} f(i\omega_n, k) = i \int_T f, \omega_n = 2\pi nT. \quad (40)$$

to take the integrals is

$$P = \int_T iD(k) = T \sum_{n=-\infty}^{\infty} \int \frac{d^3 k}{(2\pi)^2} \frac{-1}{\omega^2 - E^2} = \int \frac{d^3 k}{(2\pi)^2} \frac{1}{E} \left( \frac{1}{2} + n_B \right), \quad (41)$$

$$R = \int_T tr \ln D(k) = \int_T \ln \det D^{-1}(k) = T \sum_{n=-\infty}^{\infty} \int \frac{d^3 k}{(2\pi)^2} \left[ \ln(\omega^2 - E_1^2) + \ln(\omega^2 - E_2^2) \right] \\ = \int \frac{d^3 k}{(2\pi)^2} \left[ E_1 + 2T \ln \left( 1 - e^{-\frac{E_1}{T}} \right) + E_2 + 2T \ln \left( 1 - e^{-\frac{E_2}{T}} \right) \right], \quad (42)$$

$$\text{where } \omega = i\omega_n = 2\pi inT, E^2 = \vec{k}^2 + M^2, n_B = \frac{1}{e^{-\frac{E}{T}} - 1}, P_0 = \frac{(\mu^2)^{3/2-d/2}}{2} \int \frac{d^3 k}{(2\pi)^3} \frac{1}{E} \quad (43)$$

$$= \frac{M^2}{16\pi^2} \left( \ln \frac{M^2}{\mu^2} - 1 \right), R_0 = \frac{(\mu^2)^{3/2-d/2}}{2} \int \frac{d^3 k}{(2\pi)^3} E = \frac{M^2}{32\pi^2} \left( \ln \frac{M^2}{\mu^2} - \frac{3}{2} \right),$$

Then, we use Eq. (26), (38), (39), and Eq. (41-43) to draw the evolution of  $V^{CJT}$  (26) versus VEV  $u$  around the critical temperature  $T_c \approx 237 \text{ GeV}$ . It is plotted in Figure 2 below. The result in Fig.2 shows that the CJT effective potential ( $\tilde{V}^{CJT}$ ) is negative when  $T < T_c$ . It means that the considered model in this paper is in the broken symmetry phase when the temperature  $T < T_c$ . Furthermore, Fig.2 also shows that the  $\tilde{V}^{CJT}$  has only one minimum value when  $T < T_c$ , but this value approaches zero when  $T = T_c$ , and  $\tilde{V}^{CJT} > 0$  when  $T > T_c$ . This result proves that the phase transition in the system is of second order, occurring at  $T = T_c$ . The system transitions from a broken symmetry phase to a restored symmetry phase at the critical temperature  $T_c$ . Hence, the results in Fig.2 match the conclusion inferred from Fig.1,

confirming that the phase transition in A2HDM is of the second-order type, following the restored symmetry scenario. It must have occurred at  $T_c \approx 237\text{GeV}$ .

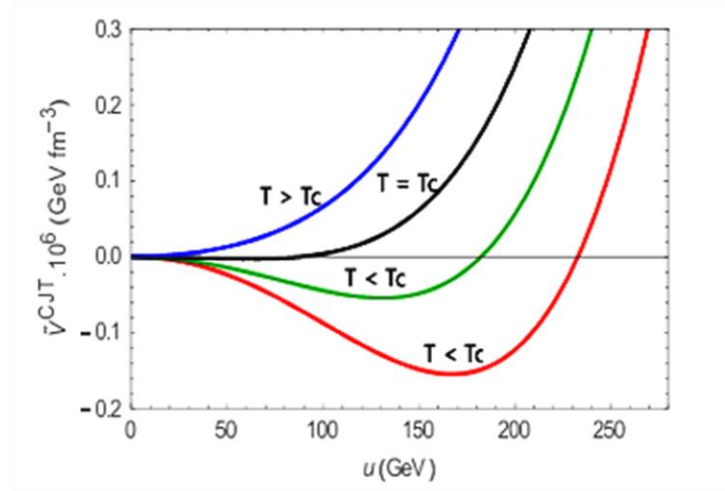


Figure 2. The dependence of  $\tilde{V}^{CJT}$  on  $u$  at some values of temperature around  $T_c$ .

### 3.2. Discussion

Since the results in Figure 1 are consistent with the LHC’s data, all the obtained results in this paper are accurate. Thus, using the CJT formalism is ready for advanced methodology and modern for studying phase transitions. On the other hand, the non-zero VEVs of two doublets in this model prove the existence of the Higgs particles with determined masses. To make this conclusion more precise, based on Eq.(37), we consider the dependence of Higgs’s effective masses on the temperature. The result is shown in Fig. 3.

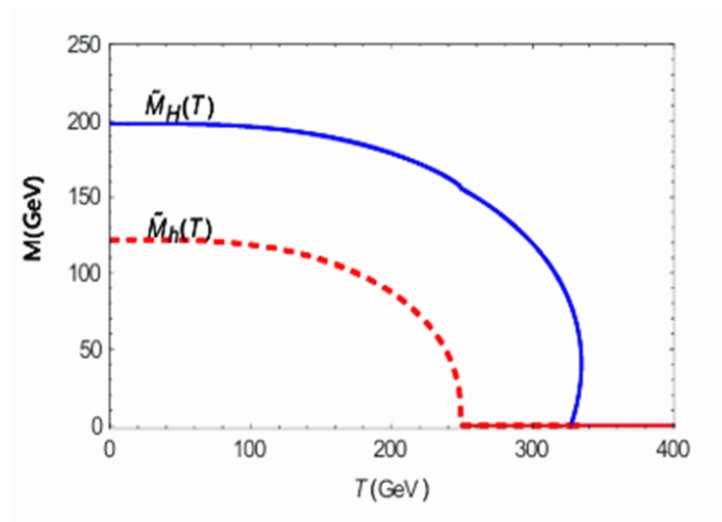


Figure 3. The  $T$  dependence of the effective masses  $\tilde{M}_h$  (the red line) and  $\tilde{M}_H$  (the blue line).

Fig. 3 shows that the effective masses of the Higgs bosons are 125 GeV and 200 GeV for the light ( $\tilde{M}_h$ ) and heavy Higgs boson ( $\tilde{M}_H$ ), respectively, at  $T \leq 100 \text{ GeV}$ . This information confirms that the phase transition is second-order in the model, following the symmetry restoration scenario again. Specifically, the mass of the light heavy Higgs is non-zero only when  $T \leq T_c \approx 237 \text{ GeV}$ , the mass of the heavy Higgs exists at a higher temperature  $T \leq 340 \text{ GeV}$ . However, we have not reached this temperature in the Lab. Therefore, the results can suggest an experimental process for detecting the existence of the Higgs boson.

In this paper, we have found that the phase transition in the A2HDM is second-order when the CJT effective potential is renormalized to preserve the Goldstone theorem, while the phase transition in the A2HDM is the soft first order if the CJT effective potential does not preserve the Goldstone theorem [15]. That means the results of this work confirm that the order and feature of the phase transition process in A2HDM strongly depend not only on the shape of the Higgs potential but also on the formalism used to approach the research problems. Besides, the expected scenario of the phase transition can happen by choosing suitable parameters based on the aim of the research, which is so important for numerical studies.

#### 4. Conclusions

In this work, we investigate the order and scenario of phase transition in A2HDM, which prevents the mixing of  $h$ - $H_0$  and satisfies the Goldstone theorem by using the CJT effective potential formalism approach in the double-bubble approximation at finite temperature. The main results we found are in order:

- We found that the CJT effective potential preserved the Goldstone theorem for ATHDM.
- The phase transition in the ATHDM is second-order and occurs following the symmetry restoration scenario.
- We prove that the masses of the Higgs boson in the model are determined and match the LHC's data.

#### References

- [1] ATLAS Collaboration, Observation of a New Particle in the Search for the Standard Model Higgs boson with the ATLAS detector at the LHC, Phys. Lett. B, Vol. 716, 2012, pp. 1-29, <https://doi.org/10.1016/j.physletb.2012.08.020>.
- [2] ATLAS, G. Aad et al., Beyond Standard Model Higgs Boson Searches at a High-Luminosity LHC with ATLAS, 2013.
- [3] ATLAS Collaboration, Ljiljana Morvaj\*, Searches for BSM Higgs Bosons in ATLAS, POS EPS-HEP2019, Vol. 584, 2020.
- [4] ATLAS, G. Aad et al., A Search for the Dimuon Decay of the Standard Model Higgs Boson with the ATLAS Detector, Phys. Lett. B, Vol. 812, 2021, pp. 135980.
- [5] The ATLAS and CMS Collaborations, and Phys. Rev. Lett, Evidence for the Higgs Boson Decay to a  $Z$  Boson and a Photon at the LHC, Vol. 132, 2024, <https://doi.org/10.1103/PhysRevLett.132.021803>.
- [6] The ATLAS Collaboration, Observation of Gauge Boson Joint-polarization States in  $W \pm Z$  Production from  $p p$  Collisions at  $\sqrt{s} = 13 \text{ TeV}$  with the ATLAS Detector, Phys. Lett. B, Vol. 843, 2023, pp. 137895, <https://doi.org/10.1016/j.physletb.2023.137895>.
- [7] ATLAS Collaboration, Characterising the Higgs Boson with ATLAS Data from Run 2 of the LHC, Physics Reports, 2024, <https://doi.org/10.48550/arXiv.2404.05498>.
- [8] S. Iguro, T. Kitahara, Y. Omura, H. Zhang, Chasing the two-Higgs Doublet Model in the di-Higgs Boson Production, Physical Review D, Vol 107, 2023, pp. 075017, <https://doi.org/10.1103/PhysRevD.107.075017>.

- [9] ATLAS, M. Aaboud et al., Observation of Higgs Boson Production in Association with A Top Quark Pair at the LHC with the ATLAS detector, *Phys. Lett. B* 784, 173, 1806.00425, 2018.
- [10] R. Kanishka, D. Indumathi, Lakshmi S. Mohan, V. Bhatnagar, Simulation Analysis with Rock Muons from Atmospheric Neutrino Interactions in the ICAL Detector at the India-based Neutrino Observatory, *The European Physical Journal C, Eur. Phys. J. C*, Vol. 83, No. 1089, 2023, <https://doi.org/10.1140/epjc/s10052-023-12133-2>.
- [11] T. Moii, C. S. Lim, S. N. Mukherjee, *The Physics of the Standard Model and Beyond*, World Scientific, 2004, ISBN: 9789810245719, 9810245718.
- [12] A. M. Sirunyan et al., Evidence for Higgs Boson Decay to a Pair of Muons, *JHEP*, Vol. 01, No. 148, 2021, pp. 04363.
- [13] D. Fontes, *Multi-Higgs Models: Model Building, Phenomenology and Renormalization*, PhD thesis, 2020, arXiv: hep-ph/2109.08394.
- [14] D. T. Tam, D. T. M. Hue, N. T. Anh, Phase Transition of the Aligned Two-higgs-doublet Model in the Cornwall – Jakiv- Tomboulis formalism, *Nuclear Science and Technology*, Vol. 12, No. 4, 2023, pp. 47-54.
- [15] J. M. Cornwall, R. Jackiw, E. Tomboulis, *Effective Action for Composite Operators*, *Phys. Rev. D*, Vol. 10, 1974. pp. 2428.
- [16] J. Goldstone, A. Salam, and Weinberg, *Broken Symmetries*, *Phys. Rev.*, Vol. 127, No. 965, 1962.
- [17] L. D. Landau, E. M. Lifshitz, *Statistical Physics*, Pergamon Press, Oxford, 1987.
- [18] M. Aoki, T. Komatsu, H. Shibuya, *Prog. Theor. Exp. Phys.*, 063B05, 2022.